

## **EFFECT OF ROUND CORNERS ON BOWTIE ANTENNAS**

**S. W. Qu and C. L. Ruan**

Institute of Applied Physics  
University of Electronic Science and Technology of China (UESTC)  
Chengdu, China

**Abstract**—In this paper, three types of novel bowtie antennas with round corners are presented and studied carefully, including quadrate, rounded-edge and triangular shapes, which have better return loss, flatter input impedance, more stable radiation patterns and smaller area at the same time. The effect of round corners is attached importance to due to their novelty. The conclusion is drawn that adding the round corners at the sharp vertexes of radiation surfaces can have positive effects on performances of not only bowtie antennas but also the others.

### **1. INTRODUCTION**

Much attention has been paid to ultra wide band (UWB) systems in which UWB antennas are the important components. As one of UWB antennas, bowtie antennas fed by coaxial line [1, 2], coplanar waveguide [3, 12] and stripline [4], have many advantages, such as low profile, ultra wide impedance band, high radiation efficiency and easy to manufacture etc. They are used in many domains due to the advantages mentioned above, such as ground penetrating radar [6–8] and pulse antennas [1, 2, 9]. However, the patterns of bowtie antenna are not ideal in full impedance band for pulse exciting, because they are distorted greatly in high frequency, and its scale is large at the same time. In paper [1], the stable patterns from 1.2 GHz to 3 GHz and wide impedance bandwidth are obtained by RC-loaded but the efficiency is reduced greatly. Bowtie antenna with a circle cap is designed and fabricated in paper [5], but its reflection coefficient in higher frequency is poor because of the matching network.

In this paper, the performances of three types of bowtie antennas, quadrate, rounded-edge and triangular shapes, are improved by adding

round corners on their radiation surfaces. The better return loss, flatter input impedance and more stable radiation patterns are obtained at the same time. All results for comparison are obtained numerically and the validity of simulations is proved by experiment. All these works are used to show that putting round corners at the sharp vertexes of radiation surfaces can bring the positive effects on performances of not only bowtie antennas but also the others.

## 2. COMPARISONS AND ANALYSIS

In this section, three types of bowtie antennas, quadrate, rounded-edge and triangular shapes, are studied carefully, including input impedance, return loss and gain in normal direction. The stability of radiation patterns can be shown by gain in normal direction indirectly, which is chosen for studying the former conveniently. So the radiation patterns of every antenna are not given in detail. The effects of round corners are analyzed by comparing bowtie antennas with round corners (BARC) with ones without them (BA).

In all simulations, the substrate is not considered due to two reasons. One is for simulating simply and the other is that the emphasis of our works is researching the effect of round corners on bowtie antennas, which cannot be influenced by substrate.

To prove the validity of our numerical analysis, six antennas must be fabricated on the substrate with dielectric constant 4.4 and thickness 0.8 mm. The experimental and numerical results are compared with each other. The good agreement can prove it.

### 2.1. Quadrate Bowtie Antenna

First of all, the familiar quadrate bowtie antenna (QBA) is exemplified. Fig. 1 shows the geometry of quadrate bowtie antenna with round corners (QBARC) and the general QBA, whose sizes are listed in the caption of the figure. Fig. 1(a) and (b) have the same height  $H$  and flare angle  $\alpha$  for easy comparison. The gap distance between the upper radiation surface and below of two antennas in Fig. 1 is set to be 0.4 mm for simulation and experiment. It is obvious the former has smaller area than the latter, but it has flatter real and imaginary parts of input impedance shown by better return loss indirectly from the following analysis due to the round corners with radius  $R_1$ .

In this section, parameters  $H$  and  $\alpha$  are fixed because they have been discussed carefully in [5].  $R_1$  is attached importance to mainly due to its novelty. Fig. 2 shows the input impedance and return loss of

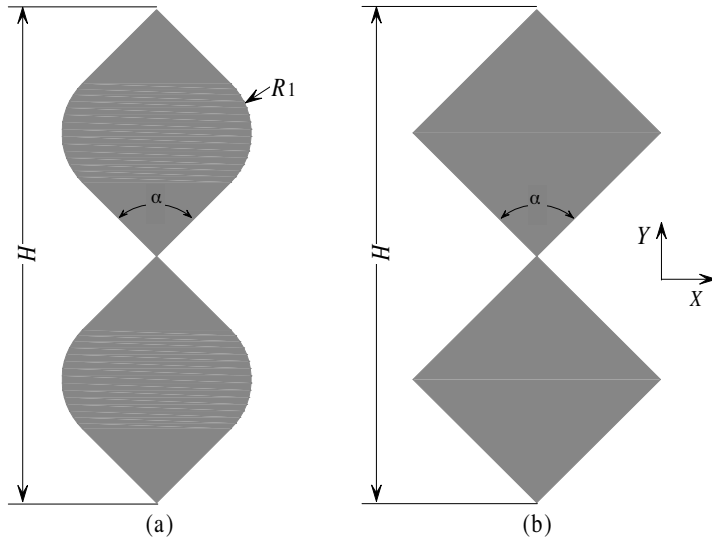


**Figure 1.** (a) QBARC. (b) QBA.  $H = 70.7$  mm,  $\alpha = 90^\circ$ .

QBA and QBARC with different  $R_1$ . All numerically studied antennas in this section are matched to  $188.5\Omega$ .

In Fig. 2, the imaginary and real parts of input impedance of QBARC are flatter than QBA. However, the antenna area decreases with  $R_1$  increasing, which causes the first resonance rise slightly but does not influence the lowest frequency for  $S_{11} \leq -10$  dB. The best return loss occurs when  $R_1 = 12$  mm.

Gain in  $Z$ -axis direction can show the stability of radiation patterns. As far as the bowtie antennas are concerned, the flatter the gain in  $Z$ -axis direction is, the more stable the radiation patterns are. The existence of round corners influences the radiation patterns strongly, especially in high frequency. In Fig. 3, gain in  $Z$ -axis direction of QBARC with  $R_1 = 12$  mm is enhanced over 10 dB than QBA except a small band near 8 GHz.

The existence of round corners does not change the average input impedance of QBARC, but makes it flatter and then the better return loss is obtained. The existence of round corners decreases the area of QBARC, but its impedance bandwidth is not changed obviously.

These improvements can be explained as follows. Round corners at the sharp vertexes of QBARC decreases the reflection of incident current near the edges and changes the current distribution on radiation surfaces compared with QBA, for example, in Fig. 4 at 3 GHz, and the radiation patterns, return loss and input impedance

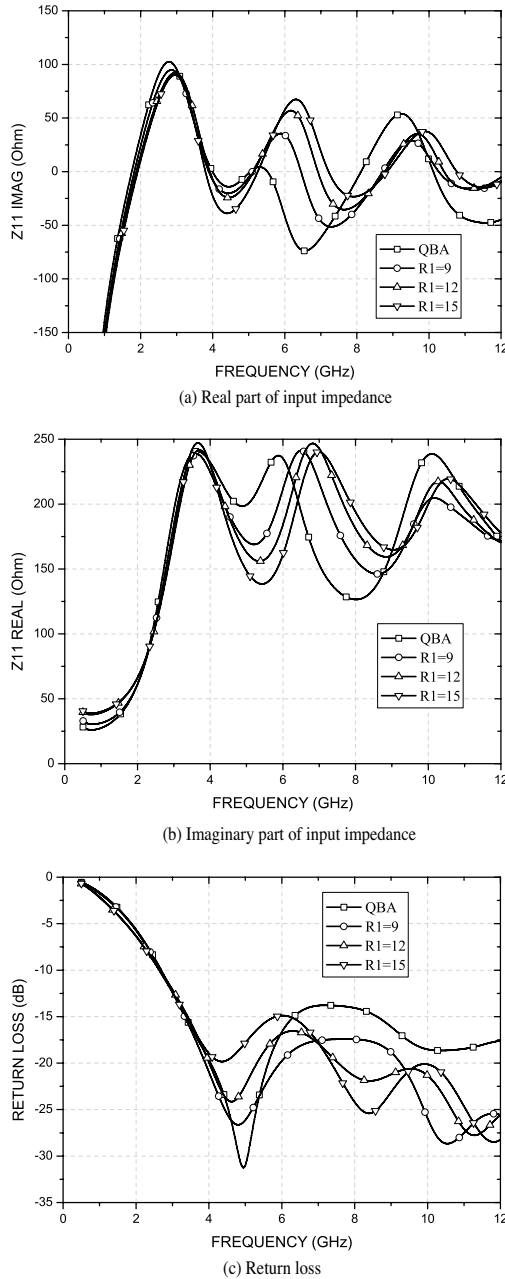


**Figure 2.** Comparison of input impedance and return loss between QBA and QBARC with different  $R_1$  (in mm).  $H = 70.7$  mm,  $\alpha = 90^\circ$ .

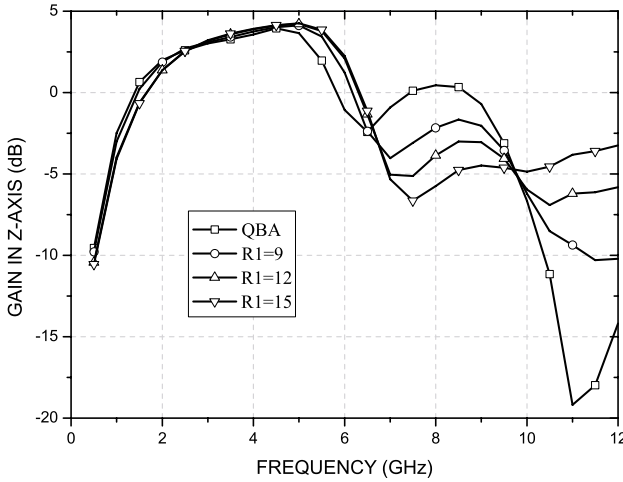


**Figure 3.** Gain in  $Z$ -axis direction of QBA and QBARC with different  $R_1$  (in mm).  $H = 70.7$  mm,  $\alpha = 90^\circ$ .

are improved subsequently. This method is also used in [11] to obtain wider impedance band.

The mirror method is used to measure the QBARC and QBA fed by  $50\ \Omega$  coaxial transmission line. The antennas are fabricated on the substrate with dielectric constant 4.4 and thickness 0.8 mm and their parameters are shown in Fig. 5, and measured by 10 MHz–20 GHz ZVM of R&S. The numerical and experimental results are given in Fig. 6, and the finite ground plane instead of the infinite and inaccurate dielectric constant of substrate cause the disagreement. The return loss of QBARC has 2 dB improvement than QBA on average.

## 2.2. Rounded-edge Bowtie Antenna

Secondly, the rounded-edge bowtie antenna (REBA) is exemplified. It is used extensively in many domains, such as pulse-exciting antennas [1, 2, 9], ground-penetrating radar [8]. Fig. 7 shows the rounded-edge bowtie antenna with round corners (REARC) and REBA. Cutting away two round corners with the same radius  $R_2$  at the top sharp vertexes of REBA forms the REARC. The two antennas has the same height  $L$  and flare angle  $\beta$  for comparing the effect of round corners easily, which are fixed that  $L = 70.7$  mm and  $\beta = 90^\circ$  because they have been studied carefully in [8]. The substrate supporting the radiation surfaces is not considered due to the reason at the beginning of Section 2. The gap distance between the upper radiation surface

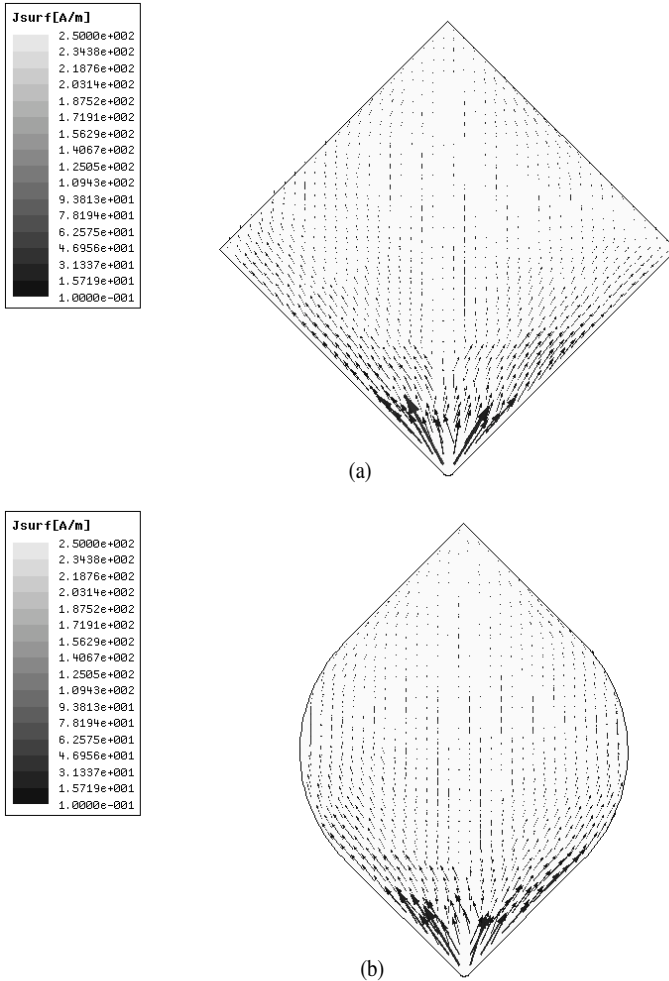
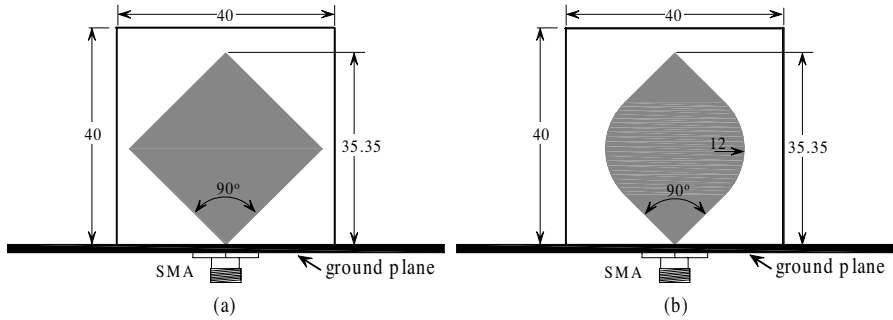


**Figure 4.** Current distribution on radiation surface at 3 GHz.  $H = 70.7$  mm,  $\alpha = 90^\circ$ ,  $R_1 = 12$  mm. (a) QBA. (b) QBARC.

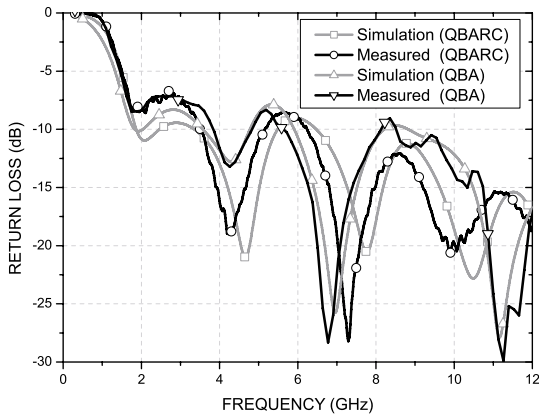
and below is set to be 0.4 mm for simulation and experiment.

Fig. 8 shows the input impedance and return loss of QBA and QBARC with different  $R_2$ . All numerically studied antennas in this section are matched to  $188.5 \Omega$ .

In Fig. 8, the input impedance of REARC becomes flatter and then steeper with increase of  $R_2$ , and at the same time the first resonance rises due to the area decrease of REARC. However, the input



**Figure 5.** Fabricated antennas. All parameters in millimeter. (a) QBA. (b) QBARC.



**Figure 6.** Measured and numerical results of QBARC and QBA.

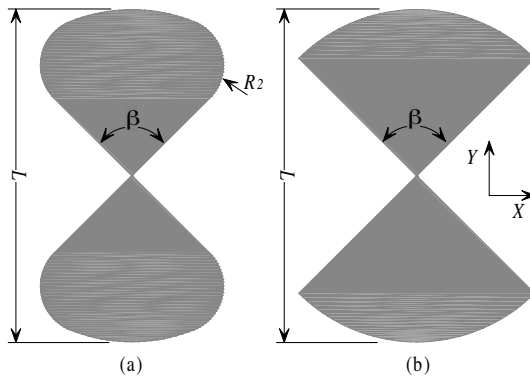
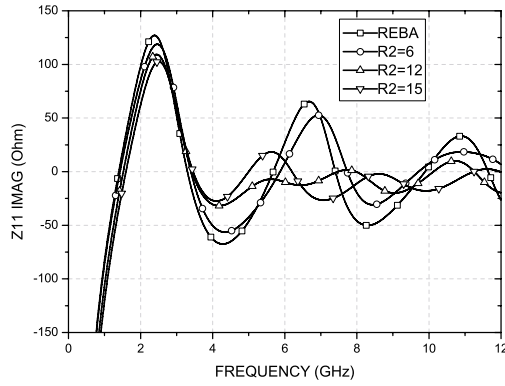
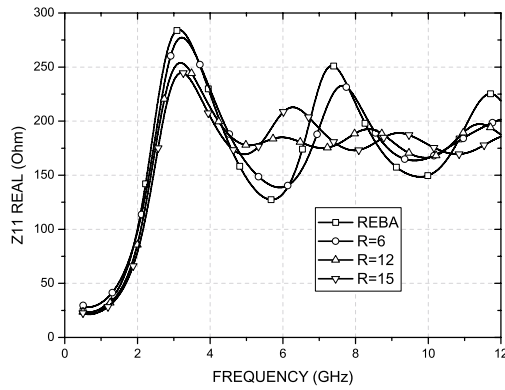


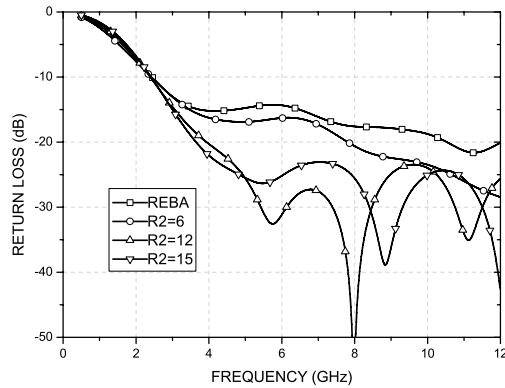
**Figure 7.** (a) REARC. (b) REBA.  $L = 70.7$  mm,  $\beta = 90^\circ$ .



(a) Imaginary part of input impedance



(b) Real part of input impedance



(c) Return loss

**Figure 8.** Comparison of input impedance and return loss between REBA and REARC of different  $R_2$  (in mm).  $L = 70.7$  mm,  $\beta = 90^\circ$ .



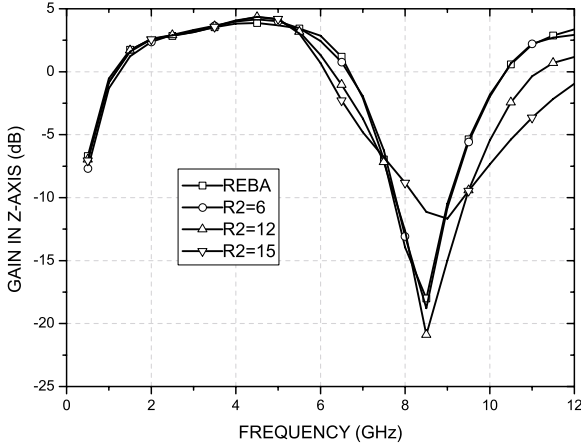


**Figure 9.** Comparison of gain in  $Z$ -axis direction between REBA and REARC of different  $R_2$  (in mm).  $L = 70.7$  mm,  $\beta = 90^\circ$ .

impedance on average is not changed, which causes the better return loss. It is exciting that the lowest frequency for  $S_{11} \leq -10$  dB does not rise obviously with increase of  $R_2$  and area decrease. The optimum  $R_2$  is equal to 12 mm.

The best gain in  $Z$ -axis direction, which shows the most stable radiation patterns, is obtained when  $R_2 = 15$  mm. It is improved close to 10 dB near 8.5 GHz. It is good for pulse-exciting antennas, which need the flat and high gain in the special direction and wide impedance band. These improvements can be explained from current distribution as in Section 2.1, which at 3 GHz is shown in Fig. 10.

To prove the validity of numerical results, the mirror method is used to measure the REARC and REBA fed by  $50 \Omega$  coaxial transmission line. The antennas are fabricated on the substrate with dielectric constant 4.4 and thickness 0.8 mm and their parameters are shown in Fig. 11, and measured by 10 MHz–20 GHz ZVM of R&S. The numerical and experimental results shown in Fig. 12 agree well with each other, and the finite ground plane instead of infinite in simulation and inaccurate dielectric constant of substrate cause the disagreement. The return loss of REARC has 3 dB improvement than REBA on average.

### 2.3. Triangular Bowtie Antenna

Third, the triangular bowtie antenna (TBA) is exemplified. This type of antenna is also used extensively in many domains, such as ground

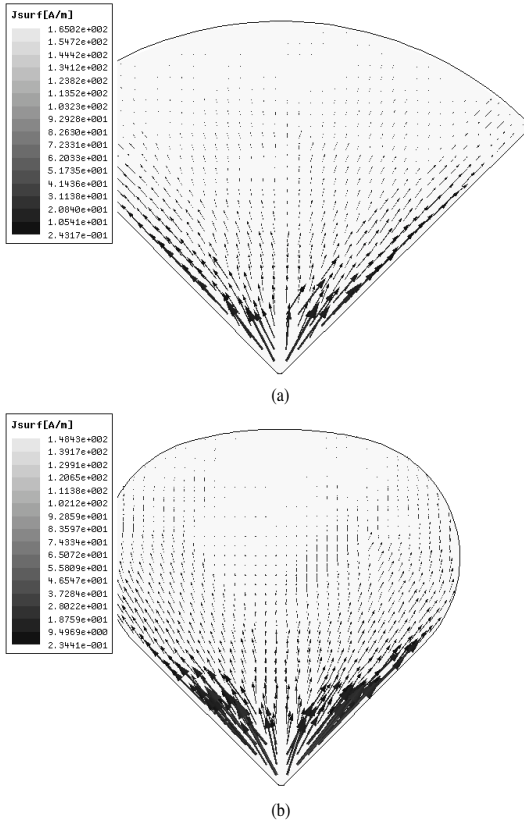


**Figure 10.** Current distribution on radiation surface at 3 GHz.  $L = 70.7$  mm,  $\beta = 90^\circ$ ,  $R_2 = 12$  mm. (a) REBA. (b) REARC.

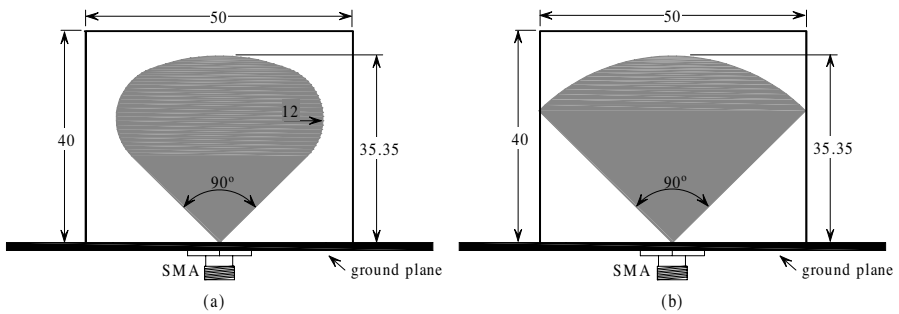


**Figure 11.** Fabricated antennas. All parameters in millimeter. (a) REARC. (b) REBA.

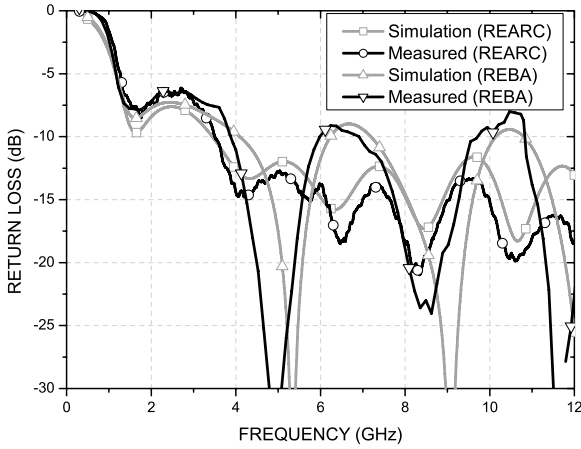


**Figure 12.** Measured and numerical results.

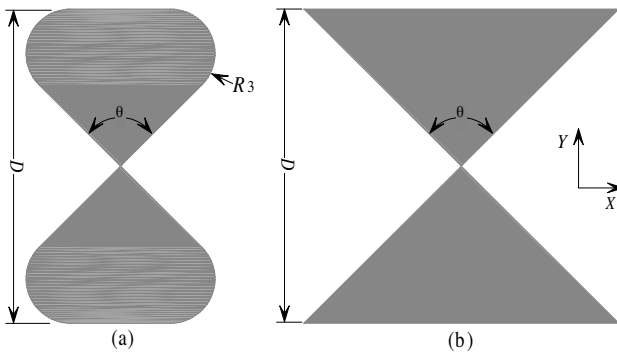
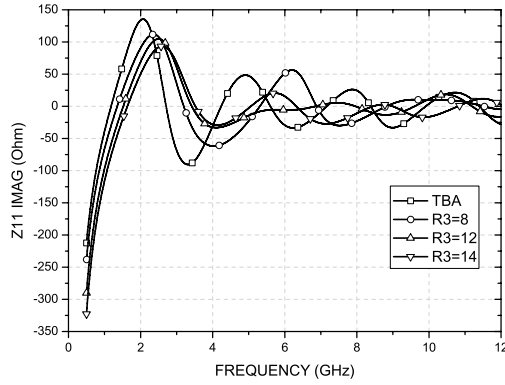


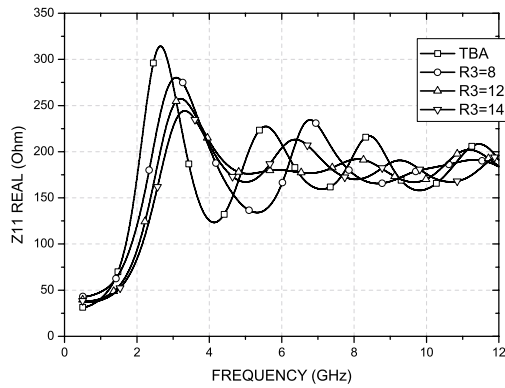
**Figure 13.** (a) TBARC. (b) TBA.  $D = 70.7$  mm,  $\theta = 90^\circ$ .

penetrating radar [6–8], mobile station [4] and Ultra wide band (UWB) communication (3.1–10.6 GHz) [10]. The geometries of triangular bowtie antenna with round corners (TBARC) and TBA are shown in Fig. 13, whose sizes are listed in the caption of the figure. Fig. 13 (a) and (b) have the same height  $D$  and flare angle  $\theta$  for easy comparison. The gap distance between the upper radiation surface and below of two antennas in Fig. 13 is set to be 0.4 mm for simulation and experiment.

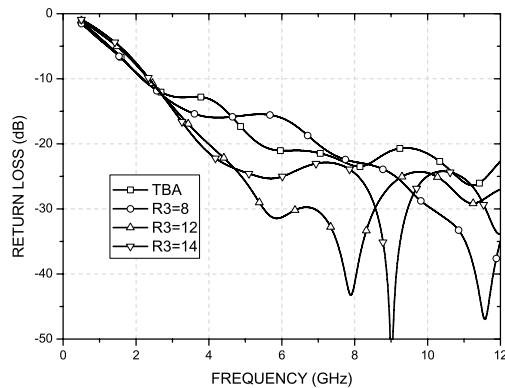
Parameters  $D$  and  $\theta$  are fixed, and  $R_3$  is studied carefully for the reasons mentioned above in Section 2.2. All numerical return losses are matched to  $188.5 \Omega$ . The numerical input impedance and return loss are shown in Fig. 14. It is obvious that the existence of round corners



(a) Imaginary part of input impedance



(b) Real part of input impedance



(c) Return loss

**Figure 14.** Comparison of input impedance and return loss between TBA and TBARC of different  $R_3$  (in mm).  $D = 70.7$  mm,  $\theta = 90^\circ$ .

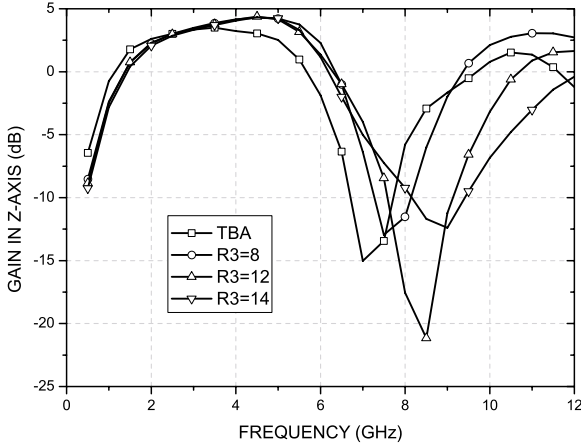


**Figure 15.** Comparison of gain in  $Z$ -axis direction between TBA and TBARC of different  $R_3$  (in mm).  $D = 70.7$  mm,  $\theta = 90^\circ$ .

does not influence the input impedance on average, and the flatness of input impedance becomes better and then worse with increase of  $R_3$  from 0 to 14 mm. The best return loss is obtained when  $R_3 = 12$  mm. However, the area of TBARC is smaller than TBA, which causes the lowest frequency for  $S_{11} \leq -10$  dB rises slightly.

Gain in  $Z$ -axis direction indicating the stability of radiation patterns is shown in Fig. 15, denoting by  $G(0, 0)$ . The below and the upper frequency band edges for  $G(0, 0) \geq 0$  dB rises at the same time and the total is not improved obviously between TBA and TBARC. When  $R_3 = 8$  mm, the gain in  $Z$ -axis direction of TBARC is better slightly. The change of current distribution brings the improvement of performances of TBARC as shown in Fig. 16.

To prove the validity of numerical results, the measurements are done using the mirror method to feed the antennas by  $50 \Omega$  coaxial transmission line, which is not restricted by frequency bandwidth. The antennas are fabricated on the substrate with dielectric constant 4.4 and thickness 0.8 mm and their parameters are shown in Fig. 17, and measured by 10 MHz–20 GHz ZVM of R&S. The numerical and experimental results shown in Fig. 18 agree well with each other, and the finite ground plane instead of infinite in simulation and inaccurate dielectric constant of substrate cause the disagreement. The return loss of TBARC has 5 dB improvement than TBA on average.

Three types of bowtie antennas are exemplified to prove the positive effect of round corners by numerical and measured results. The return loss and stability of radiation patterns are improved simultaneously

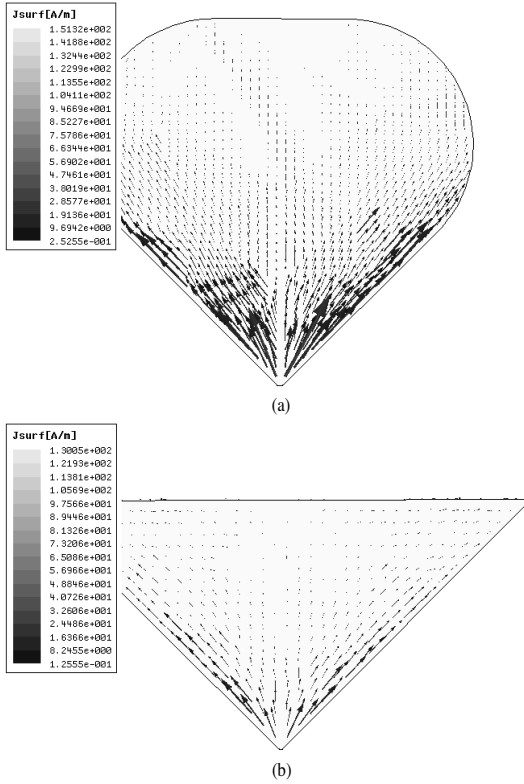


**Figure 16.** Current distribution on radiation surface at 3 GHz.  $D = 70.7$  mm,  $\theta = 90^\circ$ ,  $R_3 = 12$  mm. (a) TBARC. (b) TBA.

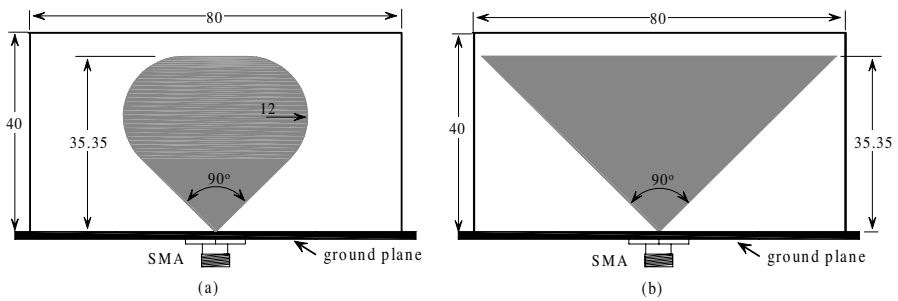


**Figure 17.** Fabricated antennas. All parameters in millimeter. (a) TBARC. (b) TBA.

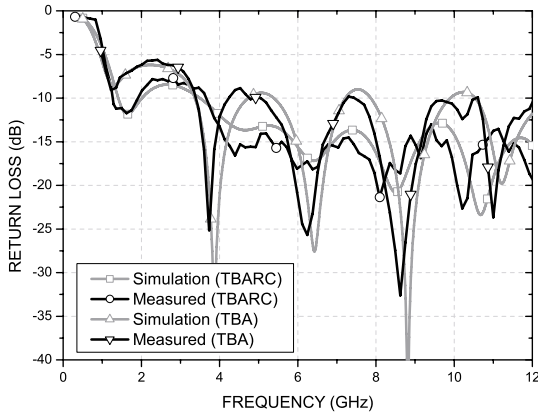


**Figure 18.** Measured and numerical results of TBARC and TBA.

by changing the current distribution on radiation surface due to the existence of round corners. For widening impedance band, resistance-loading, RC-loading and different feeding technologies are used [1, 2, 4, 6–10]. However, the efficiency reduces greatly due to loading and the volume is enlarged greatly at the same time. Different feeding technologies cannot exhibit the best performance of bowtie antennas. The efficiency of bowtie antennas with round corners does not decrease due to none loading, and their areas are reduced and the better return loss and more stable patterns are obtained at the same time.

The authors think round corners at the sharp vertexes of radiation surface have positive effect not only on bowtie antennas but also the others. However, the paper about it is not seen infrequently. In [11], the impedance bandwidth is enhanced greatly by adding four round corners at the four vertexes of rectangular slot on the ground plane, which gives a good proof of this idea.

### 3. CONCLUSION

Three types of novel bowtie antennas with round corners are proposed in the paper. The effects of round corners on the input impedance and return loss have studied carefully. The existence of round corners improves the return loss and flatness of input impedance and can enhance the stability of radiation patterns more or less at the same time. The conclusion is drawn that adding the round corners at the sharp vertexes of radiation surfaces can have positive effects on performances of not only bowtie antennas but also the others.

## ACKNOWLEDGMENT

The authors wish to acknowledge the support of Ren Wang, president of the second institute of Chengdu Yaguang Electronic Co., LTD., for measuring the proposed antennas.

## REFERENCES

1. Lestari, A. et al., "RC-loaded bow-tie antenna for improved pulse radiation," *IEEE Trans. Antennas and Propagat.*, Vol. AP-52, No. 10, 2555–2563, Oct. 2004.
2. Waldschmidt, C. and K. D. Palmer, "Loaded wedge bow-tie antenna using linear profile," *Electron. Lett.*, Vol. 37, 208–209, 2001.
3. Cantrell, W. H. and W. A. Davis, "A modified bow-tie slot antenna fed by a coplanar waveguide," *IEEE AP-S Symposium*, Vol. 1, 799–802, Jun. 2004.
4. Lin, Y.-D. et al., "Analysis and design of broadside-coupled striplines-fed bow-tie antennas," *IEEE Trans. Antennas and Propagat.*, Vol. AP-46, No. 3, 459–460, Mar. 1998.
5. Saitou, A. et al., "Practical realization of self-complementary broadband antenna on low-loss resin substrate for UWB application," *IEEE Microwave Symposium Digest, MTT-S International*, Vol. 2, 1263–1266, Jun. 2004.
6. Uduwawala, D. et al., "A deep parametric study of resistor-loaded bow-tie antennas for ground penetrating radar applications using FDTD," *IEEE Trans. Geoscience and Remote Sensing*, Vol. 42, No. 4, 732–742, Apr. 2004.
7. Nishioka, Y. et al., "FDTD analysis of resistor-loaded bow-tie antennas covered with ferrite-coated conducting cavity for subsurface radar," *IEEE Trans. Antennas and Propagat.*, Vol. 47, No. 6, 970–977, Jun. 1999.
8. Birch, M. and K. D. Palmer, "Optimized bow-tie antenna for pulsed low-frequency ground-penetrating radar," *Proceeding of SPIE*, Vol. 4758, 2002.
9. Shlager, K. L. et al., "Optimization of bow-tie antennas for pulse radiation," *IEEE Trans. Antennas and Propagat.*, Vol. 42, No. 7, 975–982, Jul. 1994.
10. Kiminami, K. et al., "Double-sided printed bow-tie antenna for UWB communications," *IEEE Antennas and Propagat. Lett.*, Vol. 3, 152–153, 2004.
11. Lee, H.-L. et al., "Broadband planar antenna having round corner



- rectangular wide slot,” *IEEE Antenna and Propagation Society International Symposium*, Vol. 2, 460–463, Jun. 2002.
12. Eldek, A. A. et al., “Characteristics of bow-tie slot antenna with tapered tuning stubs for wideband operation,” *Progress In Electromagnetics Research*, PIER 49, 53–69, 2004.